JACS
JOURNAL OF THE AMERICAN CHEMICAL SOCIETY
Article
pubs.acs.org/JACS

Dramatically Promoted Swelling of a Hydrogel by Pillar[6]arene–Ferrocene Complexation with Multistimuli Responsiveness

Mengfei Ni, Ning Zhang, Wei Xia, Xuan Wu, Chenhao Yao, Xin Liu, Xiao-Yu Hu, Chen Lin,* and Leyong Wang*

Key Laboratory of Mesoscopic Chemistry of MOE, Collaborative Innovation Center of Chemistry for Life Sciences, School of Chemistry and Chemical Engineering, Nanjing University, Nanjing, 210023, China

Supporting Information

ABSTRACT: The swelling–shrinking transition of hydrogels is crucial for their wide applications such as actuators and drug delivery. We hereby fabricated a smart hydrogel with ferrocene groups on pendant of polymer networks. While it was immersed in the water-soluble pillar[6]arene (**WP6**) aqueous solution, the hydrogel was dramatically swollen, which was an approximately 11-fold promotion in weight compared with that in pure water, due to the formation of the inclusion complexes between **WP6** and ferrocene groups in the hydrogel. In particular, the well-swollen hydrogel exhibited good responsiveness to multistimuli including temperature, pH, redox, and competitive guests by tuning the dissociation/formation of **WP6**–ferrocene inclusion complexes or the strength of their charges. Meanwhile, potential application of such a smart hydrogel in pH-responsive drug release was demonstrated as well.

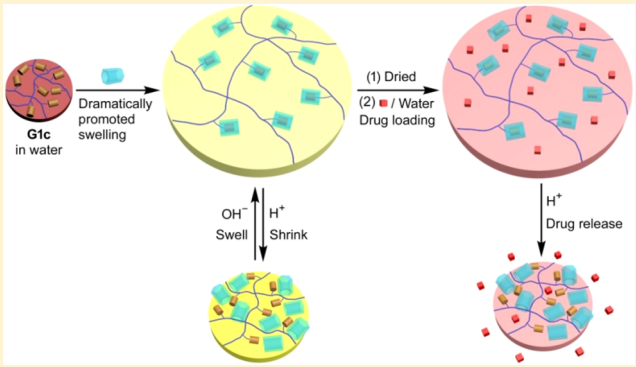

1. INTRODUCTION

In recent years, hydrogels, a type of hydrophilic three-dimensional polymeric networks,[1] have been extensively studied because of their outstanding characteristics and wide applications in bioscience and material science.[2] Among all the characteristics of hydrogels, the absorption and storage of water is basic and also significant. Especially, the water absorption is accompanied by the shape and volume changes of hydrogels. Generally, hydrogels swell with water absorption and shrink with water release. A special type of hydrogels is named smart hydrogels, whose swelling–shrinking behaviors are responsive to external stimuli including temperature, pH, light, electric, and pressure.[2c] This type of hydrogels has also been widely applied in fields such as actuator,[3] drug delivery,[2c,4] and protein protection.[5]

Host–guest interactions have become one of practical and popular interactions in the construction of supramolecular polymers with various functions[6] and self-healing materials,[7] polymer blending,[8] supramolecular adhesion,[9] and control of the lower critical solution temperature (LCST) of thermoresponsive polymers[10] in recent years. However, only a few attempts have been made to control the swelling–shrinking behaviors of hydrogels in macroscopic scale by host–guest interactions, which were utilized as shape-memory polymers,[11] artificial muscles,[12] and actuators.[13] In these cases, the swelling–shrinking transition of hydrogels was either in small degree or did not efficiently exhibit responsiveness to external multistimuli. Thus, the realization of large degree of swelling–shrinking transition of hydrogels in macroscopic scale with multistimuli responsiveness by host–guest interactions is still a big challenge. Herein, we report a smart hydrogel whose swelling ratio could be dramatically promoted by host–guest interaction based on a macrocycle named pillar[*n*]arene,[14] and the well-swollen hydrogel showed good multistimuli responsive behaviors.

The water-soluble pillar[6]arene (**WP6**) contains a hydrophobic cavity and hydrophilic carboxylates distributed on both rims of the macrocycle (Figure 1). This unique structure endows **WP6** strong hydrophilicity and excellent solubility in water, together with strong incorporation of the hydrophobic guest moiety in its cavity by hydrophobic effect.[15] We previously reported the host–guest interactions between pillar[6]arene and ferrocene (or ferrocenium) as well as its derivatives in organic or aqueous solution.[15b,16] The strong binding ability between **WP6** and ferrocene derivatives with multistimuli responsiveness motivated us to develop a novel type of smart hydrogels based on their host–guest interaction. In the present work, we prepared a polymer network **G1c** with pendant ferrocene groups (Figure 1), and while **G1c** was immersed in **WP6** aqueous solution, a dramatically well-swollen **G1c**·**WP6** hydrogel was achieved, which was an approximately 11-fold promotion in weight compared with that in pure water. The reason is that the inclusion complexes between **WP6** and

Received: March 30, 2016
Published: May 9, 2016

DOI: 10.1021/jacs.6b03296
J. Am. Chem. Soc. 2016, 138, 6643–6649

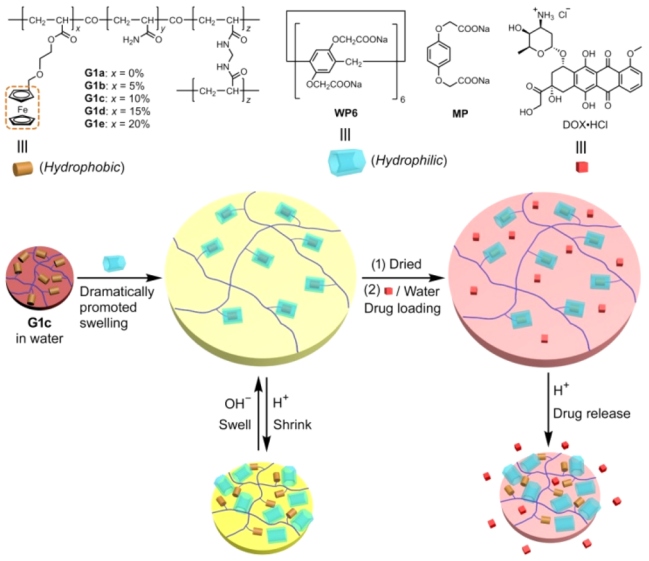

Figure 1. Structures of polymer networks **G1**, **WP6**, **MP**, and doxorubicin hydrochloride (DOX·HCl); Illustration of the dramatically promoted swelling of **G1c** by **WP6**–ferrocene host–guest interactions, and subsequently pH-responsive swelling–shrinking transition and application in controlled drug (DOX·HCl) release.

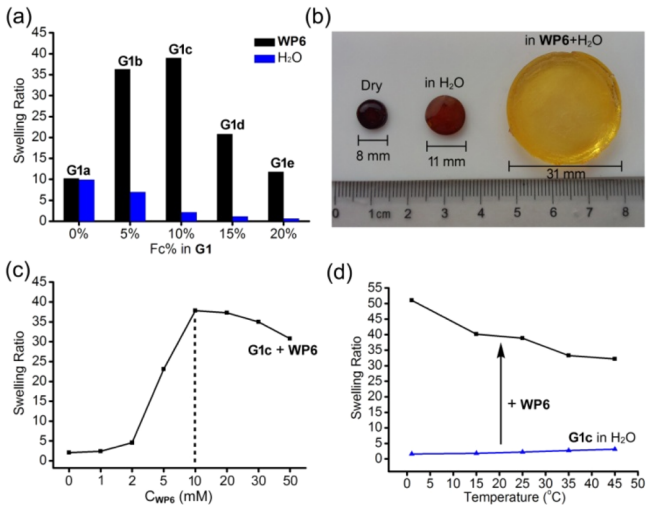

Figure 2. (a) Swelling ratio of **G1a**–**G1e** immersed in pure water and **WP6** aqueous solution (10 mM) at 25 °C, respectively. (b) Photographs of **G1c** hydrogels before and after immersed in pure water and in **WP6** aqueous solution (10 mM) at 25 °C, respectively. (c) Swelling ratio of **G1c** immersed in **WP6** aqueous solution at different **WP6** concentration at 25 °C. (d) Swelling ratio of **G1c** immersed in pure water and **WP6** aqueous solution (10 mM) at different temperature, respectively.

ferrocene groups of **G1c** were formed, which transformed the hydrophobic ferrocene groups into hydrophilic moieties[11] and meanwhile generated strong electrostatic repulsion between polymer chains due to the negatively charged carboxylates of **WP6**. The **G1c·WP6** hydrogel showed good responsiveness to external multistimuli including temperature, pH, redox, and competitive guests by tuning the dissociation/formation of **WP6**–ferrocene inclusion complexes or the strength of their charges. Meanwhile, the potential application of such a smart hydrogel in controlled drug release through the pH-tuned dissociation of **WP6**–ferrocene inclusion complexes was demonstrated as well. To the best of our knowledge, this is the first example of a smart hydrogel with excellent swelling–shrinking behaviors based on the host–guest interaction of pillar[6]arene and ferrocene.

2. RESULTS AND DISCUSSION

Swelling Promotion of Hydrogels by WP6–Ferrocene Complexation. We first confirmed the **WP6**–ferrocene complexation in D_2O between **WP6** and a linear random copolymer **P1** containing 10 mol % ferrocene subunits and 90 mol % acrylamide subunits (Figure S7–S9). Then a series of disc-shaped samples consisting of cross-linked random copolymers **G1** (Figure 1) were prepared by free radical copolymerization of a mixture of a ferrocene modified monomer, acrylamide, and *N*,*N*′-methylenebis(acrylamide) in DMSO in vials (see Supporting Information). The molar ratio of ferrocene subunit (x) of **G1** differed in a range of 0 to 20 mol % (**G1a**–**e**), while the molar ratio of cross-linker *N*,*N*′-methylenebis(acrylamide) (z) was kept constant at 0.5 mol %.

Initially, the swelling behaviors of **G1a**–**e** with different molar ratio of ferrocene subunit (x) were systematically investigated. Because of the hydrophobic ferrocene groups, the swelling ratio of **G1a**–**e** immersed in pure water obviously decreased as the molar ratio of ferrocene subunits increased from 0% (**G1a**) to 20% (**G1e**) as shown in Figure 2a. However, the immersion of **G1b**–**e** in **WP6** aqueous solution (10 mM) dramatically promoted their swelling ratio, and **G1a** without any ferrocene subunit (0%) on polymer network did not greatly swell. This swelling phenomenon in **WP6** aqueous solution could be explained by the formation of the inclusion complexes between **WP6** and ferrocene groups of **G1b**–**e**, which transformed the hydrophobic ferrocene groups into hydrophilic moieties and meanwhile generated strong electrostatic repulsion between polymer chains due to the negatively charged carboxylates of **WP6**. Moreover, with initially increasing molar ratio of ferrocene subunit from 0% (**G1a**) to 10% (**G1c**), the swelling ratio of hydrogels was increasing, but followed by the continually increasing molar ratio of ferrocene subunit from 10% (**G1c**) to 20% (**G1e**), the swelling ratio of hydrogels was decreasing. The reason is that more ferrocene subunits contained in a hydrogel assisted to grasp more **WP6** into the polymer network, which led to the higher swelling ratio of **G1c** than that of **G1b**, and on the other hand, the polymer network could not hold much more **WP6** with the increasing molar ratio of ferrocene subunits in **G1d**–**e** due to the electrostatic repulsion between negatively charged **WP6**. Therefore, when the molar ratio of ferrocene subunits was larger than 10%, the hydrophobic effect induced by ferrocene groups began to play the dominant role, which resulted in the lower swelling ratio of **G1d**–**e** compared with **G1b**–**c**.

As a result, **G1c** hydrogel, which showed the greatest swelling ratio in **WP6** solution, was selected to investigate the diameter changes of dried hydrogel before and after immersed in pure water and in **WP6** aqueous solution at 25 °C, respectively (Figure 2b). When dried **G1c** was immersed in pure water until the swelling equilibrium was reached, the diameter of the disc only increased 37% from 8 mm to 11 mm. However, when dried **G1c** was immersed in **WP6** aqueous solution (10 mM), the hydrogel swelled dramatically, and the diameter of the disc finally reached a maximum 31 mm, with a 287% increment compared with that of dried **G1c**. This result well demonstrated the remarkable swelling promotion of **G1c** induced by the host–guest interaction between **WP6** and the ferrocene groups

DOI: 10.1021/jacs.6b03296
J. Am. Chem. Soc. 2016, 138, 6643–6649

of polymer network. The microscopic change of **G1c** hydrogel after immersed in **WP6** aqueous solution was then investigated by scanning electron microscopy (SEM). The hydrogel immersed in pure water exhibited a heterogeneous morphology, with dense structures and porous structures in different areas (Figure 3a). The sizes of the pores also differed in a wide

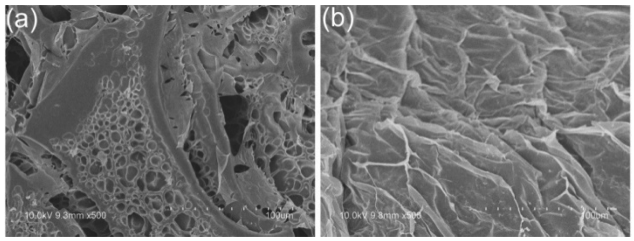

Figure 3. SEM micrographs of freeze-dried **G1c** hydrogel immersed in (a) pure water and (b) **WP6** aqueous solution (10 mM).

range. However, after sufficient swelling of **G1c** in **WP6** aqueous solution, the morphology of the hydrogel transformed to the lamellar structure (Figure 3b). This might be owing to the formation of **WP6**–ferrocene inclusion complexes, which transformed the hydrophobic ferrocene subunits into the hydrophilic moieties.

To understand the relationship between the swelling ratio of the hydrogels and different **WP6** concentration in aqueous solution, the concentration-dependent swelling behaviors of **G1c** in **WP6** aqueous solution at 25 °C were studied (Figure 2c). As the concentration of **WP6** increased from 0 mM to 2 mM, the swelling ratio of **G1c** increased slightly in the first stage, increased sharply in the second stage from 2 mM to 10 mM, and gradually decreased above 10 mM of **WP6**. The reason is that the initially increasing concentration of **WP6** resulted in the formation of more **WP6**–ferrocene host–guest binding motifs, causing the swelling of hydrogels, and, however, the high osmotic pressure in external solution induced by more **WP6** above 10 mM might result in the shrinkage of hydrogels. And then the control experiment was conducted in the aqueous solution with model compound **MP**, which is one subunit of **WP6** structure shown in Figure 1. The results (Figure S10) indicated that the swelling ratio of **G1c** immersed in **MP** aqueous solution was close to that in pure water, and kept constant roughly as the concentration of **MP** changed. This strongly supported that the host–guest interaction between **WP6** and ferrocene played an important role in the swelling of hydrogel. In addition, it was known that host–guest complexes became unstable at high temperature,[17] therefore, the swelling promotion of the hydrogels induced by host–guest interaction was supposed to be influenced by changing temperature. As expected, when the temperature increased from 1 to 45 °C, the swelling ratio of **G1c** in pure water remained almost constant, while the swelling ratio of **G1c** in **WP6** aqueous solution (10 mM) decreased obviously (Figure 2d). This phenomenon demonstrated the dethreading of the pendant ferrocene groups from **WP6** on rising temperature, which led to the shrinkage of the hydrogel.

Furthermore, polymer networks **G2**–**G4** were prepared by copolymerization of different monomers for the comparison with **G1c** (Figure 4). In the structures of **G2** (Figure 4a, x = 10%, z = 0.5%) and **G3** (Figure 4b, x = 10%, z = 0.5%) the pendant ferrocene subunits with different linkages were connected to the main chain of polymers, while in the structure

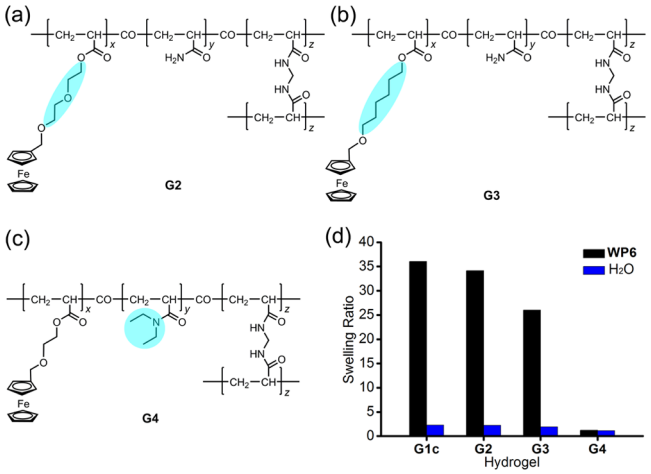

Figure 4. Structures of polymer networks: (a) **G2**, (b) **G3**, and (c) **G4**. (d) Swelling ratio of **G1c**, and **G2**–**G4** immersed in pure water, **WP6** aqueous solution (10 mM), respectively, at 25 °C.

of **G4** (Figure 4c, x = 10%, z = 0.5%) the subunit of acrylamide was replaced by *N*,*N*-diethylacrylamide compared with **G1c**. It was found that the swelling ratio of both **G2** and **G3** were promoted remarkably upon addition of **WP6** aqueous solution, regardless of the difference of the linkage between ferrocene group and polymer chain (Figure 4d). The relative lower swelling ratio of **G3** in **WP6** aqueous solution compared with **G1c** was due to the stronger hydrophobicity of the longer aliphatic chain in the pendant of **G3**. However, the swelling ratio of **G4** immersed in **WP6** aqueous solution was almost the same as that in pure water, which suggested that the strong hydrophobicity of *N*,*N*-diethylacrylamide subunit played a dominant role over the host–guest interaction.

From above results, it could be concluded that the dramatic swelling promotion of the hydrogels could be achieved by the formation of **WP6**–ferrocene inclusion complexes. Greater swelling degree would be achieved if the ferrocene groups of polymer network grasped more **WP6**. Therefore, the large association constant between the hydrophilic macrocycle and the hydrophobic pendant guest on polymer network was essential for the swelling promotion of the hydrogels. Besides, the degree of hydrophilicity of the macrocycle, especially charged macrocycle, would be another crucial factor for the swelling promotion. As for charged macrocycles, the intermolecular electrostatic repulsion would be favorable for the expansion of polymer network, but on the other hand, would be unfavorable for the host–guest interaction of the crowded pendant guests of polymer network, which therefore made the estimation of the degree of swelling promotion more difficult in comparison with neutral macrocycles, such as cyclodextrin.[11] In addition, the hydrophobic polymer backbone was also unfavorable to the swelling degree of the hydrogels promoted by host–guest interactions.

Swelling Rate of Hydrogels. The swelling rate is another important factor for the swelling behaviors of hydrogels besides the swelling ratio. We first investigated the swelling rate of **G1c** immersed in **WP6** aqueous solution (10 mM) at 25 °C, and found that it would take approximately 120 h for the swelling of the hydrogel to reach equilibrium (Figure 5). Further study revealed that the higher concentration of **WP6** in the swelling media obviously contributed to the higher swelling rate of hydrogels (Figure S11–S15). It took only about 36 h for the

DOI: 10.1021/jacs.6b03296
J. Am. Chem. Soc. 2016, 138, 6643–6649

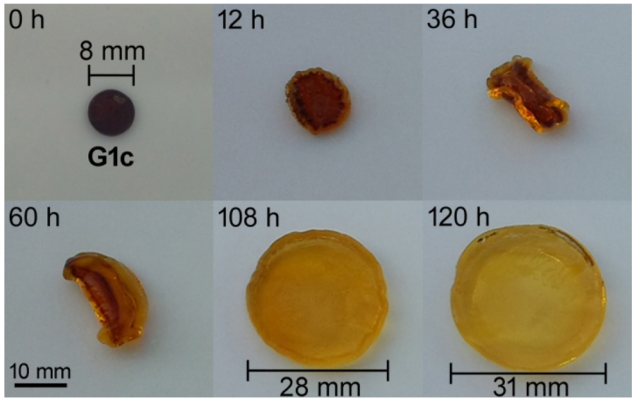

Figure 5. Photographs of **G1c** before and after being immersed in **WP6** (10 mM, 15 mL) aqueous solution at different times at 25 °C.

swelling of **G1c** to reach equilibrium when the concentration of **WP6** was 50 mM, much faster than that in 10 mM **WP6** aqueous solution in spite of the largest swelling ratio obtained in 10 mM **WP6** aqueous solution (Figure 2c), while the swelling rate in 5 mM **WP6** aqueous solution was the slowest (ca. 180 h). By comparison, the swelling of **G1c** immersed in pure water was much faster, which took only about 12 h to reach equilibrium overall. Another notable phenomenon was that the hydrogel swelled at different rates in its different disk zones in **WP6** aqueous solution, and accompanied by the volume expanding during the water absorption process, the relatively faster expanding in the disc edges made it twisty before reaching equilibrium (Figure 5, S11–S15).

The swelling rate of **G1c** in **WP6** aqueous solution was assumed to be determined by two processes: **WP6** absorption and water absorption. The **WP6** absorption process included the diffusion of **WP6** into the polymer network and subsequently binding with ferrocene groups. Since the swelling rate of **G1c** in pure water was much faster than that in **WP6** aqueous solution, it could be deduced that the **WP6** absorption process was the rate-determining step during the swelling of **G1c** in **WP6** aqueous solution. Therefore, the higher concentration (above 5 mM) of **WP6** contributed to the higher swelling rate. When the concentration of **WP6** was low enough (below 5 mM), the swelling rate became close to that in pure water, since very little **WP6** was absorbed in this condition.

Furthermore, the swelling rate of dried **G1c·WP6** hydrogel, in which **G1c·WP6** was the well-swollen hydrogel of **G1c** in **WP6** aqueous solution, in pure water was investigated (Figure S16). It was amazing that the swelling rate of dried **G1c·WP6** was dramatically promoted, and it only took approximately 2 h to complete the swelling process, superior to the swelling rates of **G1c** in pure water or **WP6** aqueous solution. Another difference was that the different disk zones of the hydrogel expanded at a similar rate and the hydrogel almost remained disc-shaped. These phenomena confirmed that **WP6** absorption process was much slower than water absorption process for the swelling of **G1c** in **WP6** aqueous solution.

Multistimuli Responsive Behaviors. The response to external stimuli was a significant property for smart hydrogels. Thanks to the reversibility of the host–guest interaction between **WP6** and ferrocene, it was workable to tune the swelling–shrinking behaviors of **G1c·WP6**.

The host–guest interaction between **WP6** and ferrocene was sensitive to pH, and the protonation of **WP6** would lead to the decomplexation of the host–guest complex.[15b] Therefore, the pH-controlled shrinking and swelling of **G1c·WP6** was first studied. The initial diameter of swollen **G1c·WP6** hydrogel in pure water (pH = 7) was approximately 35 mm (Figure 6a).

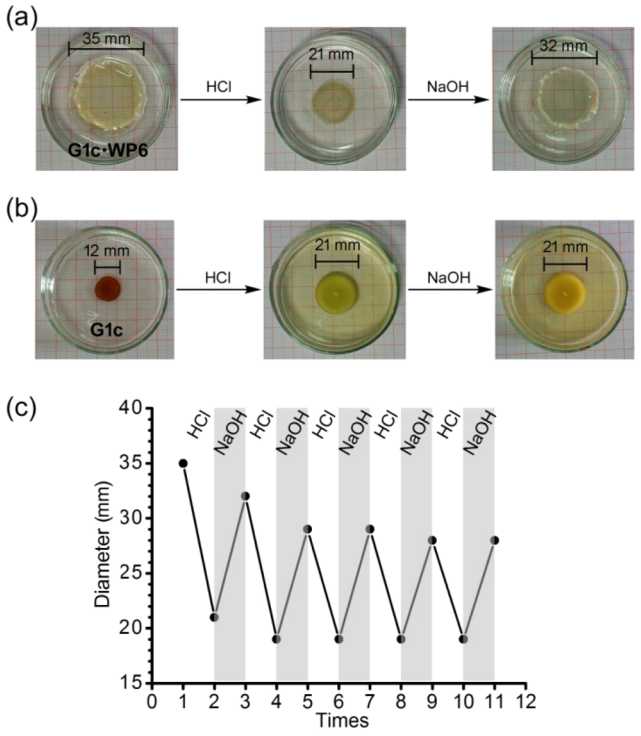

Figure 6. Photographs of hydrogels immersed in deionized water (10 mL) responsive to HCl aqueous solution (1 M, 0.1 mL, 12 h) and NaOH aqueous solution (1 M, 0.1 mL, 12 h): (a) **G1c·WP6**; (b) **G1c**. Photographs in (a, b) were taken in the swelling media. (c) Changes of the diameter of **G1c·WP6** hydrogel in (a) with the addition of HCl aqueous solution (1 M) and aqueous solution NaOH (1 M) to the swelling media, alternately (0.1 mL solution every 12 h).

When HCl aqueous solution was added to the swelling media, the hydrogel shrank gradually and the diameter decreased to a minimum 21 mm after 12 h. Subsequent addition of NaOH aqueous solution to the swelling media led to the recovery of the diameter of the hydrogel to a maximum 32 mm after 12 h. And furthermore, such a reversible cycle could be repeated for at least 5 times (Figure 6c). In the control experiment, the addition of NaCl aqueous solution to the swelling media only caused slight shrinkage of **G1c·WP6**, which was due to the increase of osmotic pressure (Figure S17). This was probably the reason why the diameter of the hydrogel in the pH-responsive experiments during cycles decreased gradually (Figure 6c). In addition, it was interesting to mention that the swelling rate of **G1c·WP6** hydrogel in the pH-controlled swelling experiments (Figure 6a), was generally faster than that of **G1c** hydrogel in Figure 5. It was due to the fact that most of the protonated **WP6** were still trapped in the polymer network when the hydrogel shrank in the presence of the acid, since little precipitation (protonated **WP6**) could be observed in the swelling media. Therefore, during the swelling process of the **G1c·WP6** hydrogel from 21 mm to 32 mm (Figure 6a), it took shorter time for the diffusion of OH^- and subsequent reaction with −COOH of protonated **WP6**, followed by the water uptake of the hydrogel, resulting in the swelling of hydrogel.

DOI: 10.1021/jacs.6b03296
J. Am. Chem. Soc. 2016, 138, 6643–6649

The pH-responsive behavior of **G1c** was quite different from that of **G1c·WP6**. After the addition of HCl aqueous solution to the swelling media (pH = 7) of **G1c**, the hydrogel swelled gradually from 12 mm to 21 mm (Figure 6b). Another notable phenomenon was that the color of the hydrogel and the swelling media became yellow green together with the appearance of yellow precipitation. This appears to be aroused from the decomposition or oxidation of partial ferrocene groups in the presence of O_2 in acid solution,[18] which made the pendants on polymer network charged and thus promoted the swelling ratio of the hydrogel. The following addition of NaOH aqueous solution to the swelling media hardly caused any change in the diameter of the hydrogel in 12 h and even longer time. If the hydrogel did not contain any ferrocene subunit (**G1a**), it would remain the appearance after the successive addition of HCl aqueous solution and NaOH aqueous solution (Figure S19a).

Then a question arose that why the ferrocene groups kept intact in acid solution in the presence of **WP6**. A possible reason was deduced from the pH change during the pH-responsive cycles of **G1c·WP6** (Figure 6a, c). The pH value of the swelling media would recover to around 7 gradually after the addition of acid and base each time in the presence of **WP6**. However, the pH value of the swelling media of **G1c** remained 2 during the 12 h after the addition of acid, and turned to 7 after the addition of equivalent base. Therefore, in this case, **WP6** could act as a buffer against the dramatic pH evolution in polymer network, which protected ferrocene groups from the unfavorable acid environment.

Ferrocene derivatives are widely applied in the construction of stimuli-responsive assemblies and materials due to their redox-responsive properties.[16b,19] Therefore, the swelling behaviors of **G1c·WP6** and **G1c** that were responsive to the redox of ferrocene groups were investigated. It was observed that **G1c·WP6** shrank gradually and the diameter decreased from 35 mm to 20 mm after the addition of $AgNO_3$ aqueous solution to the swelling media until the equilibrium was reached (Figure 7a). Then a reverse process took place when the excess hydrazine hydrate aqueous solution was added to the swelling media, which recovered the diameter of the disc to a maximum 28 mm after 24 h. Our previous study had revealed that the binding affinity between **WP6** and a ferrocenium derivative (K_a = (8.68 ± 0.72) × 10^7 M^{-1}) was much stronger than that between **WP6** and a ferrocene derivative (K_a = (1.27 ± 0.42) × 10^5 M^{-1}) in water.[15b] Therefore, the oxidization of pendant ferrocene groups could more strongly bind **WP6**, and on the other hand, the positively charged pendant ferrocenium and the negatively charged **WP6** could make the polymer network of **G1c·WP6** be a pseudozwitterionic structure, and it would prevent the expansion of the hydrogel whose previous expansion was driven by the electrostatic repulsion from a single type of charge.[20] On the contrary, **G1c** underwent a process of swelling and shrinking behaviors in response to the oxidization and reduction of ferrocene groups, respectively, with a diameter evolution from 13 mm to 23 mm, and then to 16 mm (Figure 7b). It was because the oxidization of ferrocenes would make the neutral pendant positively charged, which could increase the hydrophilicity and promote the swelling ratio of the hydrogel. In addition, as expected, **G1a** did not show the response to the addition of $AgNO_3$ and hydrazine hydrate since the hydrogel did not contain ferrocene subunits (Figure S19b, c).

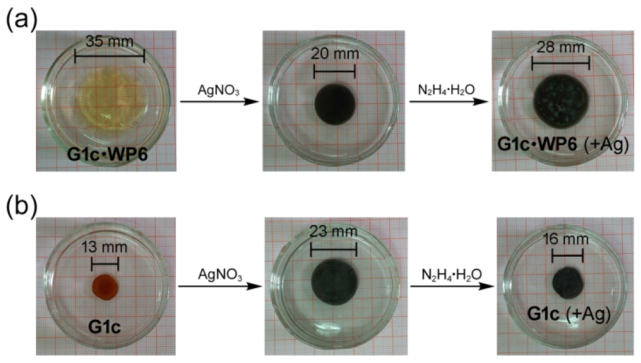

Figure 7. Photographs of hydrogels immersed in deionized water (10 mL) responsive to $AgNO_3$ aqueous solution (1 M, 0.2 mL, 24 h) and hydrazine hydrate aqueous solution (1 M, 0.5 mL, 24 h): (a) **G1c·WP6**; (b) **G1c**. Photographs in (a, b) were taken in the swelling media, with the reaction product Ag out of hydrogels removed to avoid the turbidity in some cases. The dark color of the hydrogel was owing to Ag and ferrocenium.

Host−guest interactions could also be tuned by introducing competitive guests. The reported association constant between **WP6** and *N*,*N*′-dimethyl-4,4′-bipyridinium bromide was (1.02 ± 0.10) × 10^8 M^{-1},[21] much larger than that between **WP6** and a ferrocene derivative (K_a = (1.27 ± 0.42) × 10^5 M^{-1}).[15b] Therefore, attempts were made to tune the swelling or shrinking behaviors of **G1c·WP6** by adding paraquats. The experiments revealed that the diameter of **G1c·WP6** hydrogel decreased from 36 mm to 21 mm after adding *N*,*N*′-dimethyl-4,4′-bipyridinium iodide to the swelling media until the swelling equilibrium was reached (Figure S18a). A similar shrinkage of the hydrogel could be observed as well when *N*,*N*′-dibutyl-4,4′-bipyridinium bromide was used as the competitive guest, with a diameter decrease from 36 mm to a minimum 25 mm for the hydrogel (Figure S18b). Control experiments were also carried out, which showed that **G1c** had no apparent response to paraquats in swelling ratio (Figure S19d, e).

In Vitro pH-Responsive Drug Release. The dramatic swelling−shrinking transition of the hydrogel induced by the multistimuli responsive **WP6**−ferrocene complexation provided a foundation for the application of controlled drug release. Herein, an anticancer drug doxorubicin hydrochloride (DOX·HCl) was selected as a model drug to evaluate the pH-responsive drug release behaviors of the hydrogels.

The encapsulation of DOX·HCl into the hydrogel was realized by drying the well-swollen **G1c·WP6** hydrogel and subsequently its immersion into DOX·HCl aqueous solution, in which the rapid and dramatic swelling of **G1c·WP6** was accompanied by the absorption of DOX·HCl (Figure 8). As the pH value of the release media decreased, the negatively charged carboxylates were neutralized and the hydrogel shrank gradually, accompanied by the release of encapsulated DOX·HCl. When **G1c·WP6** with loaded DOX·HCl was immersed in water (pH = 7), the cumulative leakage of DOX·HCl was less than 5% within 36 h (Figure 8). As the pH value of the release media decreased to 4, the release of DOX·HCl exhibited a gradual process, and the cumulative release percentage came to 28% after 24 h. However, in the more acidic condition (pH = 2), rapid release of DOX·HCl could be observed in the first 0.5 h, and the maximum release percentage could reach 80%, which was attributed to the faster and greater shrinkage of hydrogel in this condition. It is known that the microenvironment of tumor cells is acidic;[15c] therefore, the pH-responsive release of DOX·

DOI: 10.1021/jacs.6b03296
J. Am. Chem. Soc. 2016, 138, 6643−6649

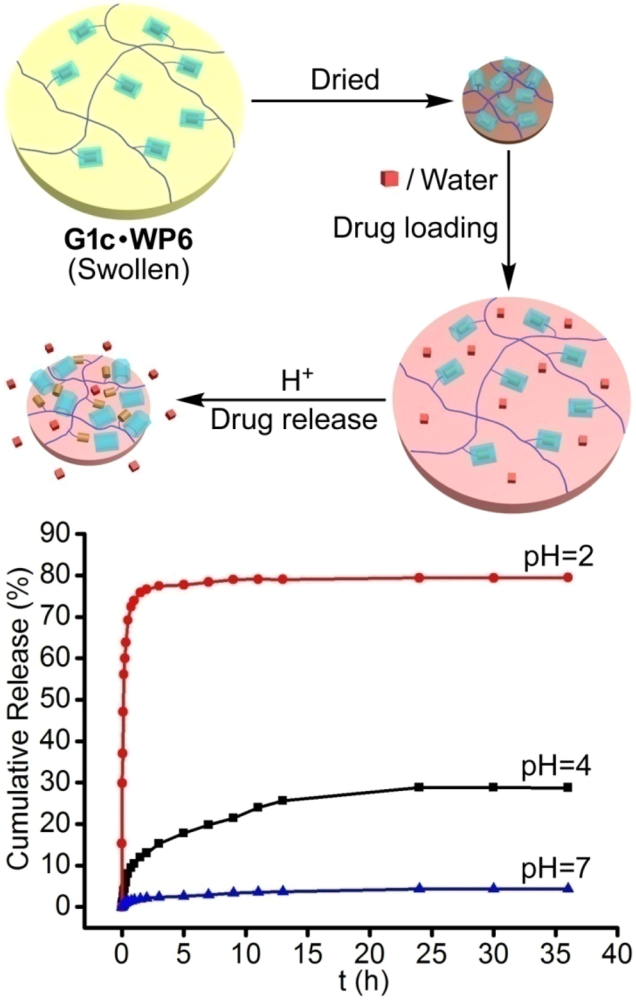

Figure 8. Illustration of the pH-responsive drug (DOX·HCl) release of **G1c·WP6** with drug loaded, and corresponding profiles of in vitro cumulative drug release in aqueous release media at different pH at 25 °C.

HCl from the hydrogel is able to be triggered in the tumor tissues. More importantly, the gradual release process under weak acidic conditions was favorable for the prolonging of administering time and the decrease of toxicity effect.

3. CONCLUSIONS

In conclusion, we have developed a smart hydrogel whose swelling ratio could be dramatically and greatly promoted with multistimuli responsiveness by host–guest interaction. Thanks to **WP6**–ferrocene complexation, the hydrogel containing 10 mol % ferrocene subunits, **G1c**, could swell 39-fold of its dried weight and 12-fold of its waterish weight without **WP6**–ferrocene complexation. This promotion was contributed by the transition of hydrophobic ferrocene groups to hydrophilic **WP6**–ferrocene inclusion complexes and additional electrostatic repulsion between negatively charged polymer chains. Besides, the swelling behaviors of **G1c·WP6** showed good multistimuli responsiveness to temperature, pH, redox, and competitive guests. Further study on the in vitro pH-responsive drug release behaviors of the hydrogel was conducted as well, which showed a potential application in controlled drug delivery. In addition, promising applications of this smart hydrogel as extractants, artificial muscles and actuators could also be foreseen.

4. EXPERIMENTAL SECTION

General Methods. All reagents were commercially available unless noted and most of them were used without further purification, except that some solvents were dried by standard methods mentioned in the synthetic procedures. **WP6**,[15a] **MP**,[22] hydroxymethyl ferrocene,[23] 2-(2-hydroxyethoxy)ethyl acrylate,[24] 6-hydroxyhexyl acrylate,[25] and *N*,*N*′-dibutyl-4,4′-bipyridinium bromide[26] were synthesized according to the literatures. All reactions were performed in atmosphere unless noted. NMR spectra were recorded on a Bruker DPX 300 spectrometer or a Bruker Avance III 400 spectrometer with TMS as the internal standard. Electrospray ionization mass spectra (ESI-MS) were acquired on a Finnigan Mat TSQ 7000 instrument. High-resolution electrospray ionization mass spectra (HR-ESI-MS) were recorded on an Agilent 6540Q-TOF LCMS equipped with an electrospray ionization (ESI) probe operating in positive-ion mode with direct infusion. Gel permeation chromatograph (GPC) analysis was performed on a PL-GPC 50 integrated GPC equipped with refractive index detector at 25 °C. The column used in the GPC analysis was PL aquagel–OH 30 8 μm 300 × 7.5 mm with DMF as the eluent. Scanning electron microscopy (SEM) was carried out on a HITACHI S-4800 device. Fluorescence spectra were recorded on a PerkinElmer LS55 Fluorescence Spectrometer.

Determination of the Swelling Ratio of the Hydrogels. In this part of experiments, the dried disc-shaped samples were immersed in 15 mL of swelling medium (deionized water, **WP6** aqueous solution or **MP** aqueous solution). After several days, the hydrogels were taken out from the swelling medium, and weighed after removing the water or solution at the surface of each hydrogel with a filer paper. Then the hydrogels were reimmersed into the swelling medium and weighted until the weight of the hydrogels was constant. The experiments were performed in a constant temperature incubator (15, 25, 35, 45 °C) or in a foam box filled with ice (1 °C, measured by a thermometer inside). Swelling ratio was calculated by the equation as follows:

$$\text{Swelling Ratio} = (W_e - W_0)/W_0$$

where W_0 is the weight of the dried hydrogel before immersed into swelling medium, and W_e is the weight of the hydrogel after the water absorption reached equilibrium. The listed swelling ratio was obtained as an arithmetic average of three measurements.

In Vitro pH-Responsive Drug Release. Dried disc-shaped **G1c·WP6** was immersed in DOX·HCl aqueous solution (5.00×10^{-4} M, 10.0 mL) in darkness at 25 °C for 12 h to absorb water and DOX·HCl. The drug-loaded hydrogel was washed with deionized water to remove the DOX·HCl aqueous solution at the surface of hydrogel before immersed in the release media. The mole of unloaded DOX·HCl was measured by a fluorescence spectrophotometer at 555 nm and calculated as relative to a standard calibration curve in the concentrations from 1.00×10^{-7} M to 2.00×10^{-5} M in water. The mole of loaded DOX·HCl was calculated by the following equations:

$$n_l = n_a - n_u$$

where n_l, n_a, and n_u represent the mole of loaded DOX·HCl, added DOX·HCl, and unloaded DOX·HCl, respectively.

The in vitro drug release experiments were carried out by immersing the drug-loaded hydrogel in 100 mL deionized water and HCl aqueous solution (pH = 2, 4) in darkness at 25 °C without stirring. At selected time intervals, 2 mL of the release media was taken out to measure the released DOX·HCl concentrations by the fluorescence technique, which was then returned to the original release media after each measurement. The concentration of DOX·HCl was determined by the measurement of emission intensity at 555 nm using a standard emission vs concentration curve constructed for DOX·HCl in the corresponding release media. The cumulative DOX·HCl release percentage was calculated by the following equation:

$$\text{Cumulative Release (\%)} = n_r/n_l \times 100$$

DOI: 10.1021/jacs.6b03296
J. Am. Chem. Soc. 2016, 138, 6643–6649

where n_r and n_l represent the mole of cumulative released DOX·HCl and loaded DOX·HCl, respectively. The listed cumulative release percentage was obtained as an arithmetic average of three measurements.

■ ASSOCIATED CONTENT

Supporting Information

The Supporting Information is available free of charge on the ACS Publications website at DOI: 10.1021/jacs.6b03296.

Synthesis and relevant characterization details, host−guest interaction study and supporting photographs. (PDF)

■ AUTHOR INFORMATION

Corresponding Authors

*linchen@nju.edu.cn

*lywang@nju.edu.cn

Notes

The authors declare no competing financial interest.

■ ACKNOWLEDGMENTS

We gratefully acknowledge the financial support of the National Basic Research Program of China (2014CB846004), National Natural Science Foundation of China (No. 21302092, 91227106, 21472089). We would like to thank Dr. Xikuang Yao and Mr. Dongliang Qi for their kind help in GPC and SEM characterization, respectively. We also thank Prof. Dongzhong Chen, Prof. Xuefeng Guo, Dr. Kun Xiang for their helpful discussion in this work.

■ REFERENCES

(1) Hennink, W. E.; van Nostrum, C. F. *Adv. Drug Delivery Rev.* **2002**, *54*, 13−36.

(2) (a) Peppas, N. A.; Sahlin, J. J. *Biomaterials* **1996**, *17*, 1553−1561. (b) Lee, K. Y.; Mooney, D. J. *Chem. Rev.* **2001**, *101*, 1869−1880. (c) Qiu, Y.; Park, K. *Adv. Drug Delivery Rev.* **2012**, *64*, 49−60. (d) Zhang, C.; Cano, G. G.; Braun, P. V. *Adv. Mater.* **2014**, *26*, 5678−5683.

(3) (a) Osada, Y.; Okuzaki, H.; Hori, H. *Nature* **1992**, *355*, 242−244. (b) Kim, Y. S.; Liu, M.; Ishida, Y.; Ebina, Y.; Osada, M.; Sasaki, T.; Hikima, T.; Takata, M.; Aida, T. *Nat. Mater.* **2015**, *14*, 1002−1007.

(4) Huffman, A. S.; Afrassiabi, A.; Dong, L. C. *J. Controlled Release* **1986**, *4*, 213−222.

(5) Beierle, J. M.; Yoshimatsu, K.; Chou, B.; Mathews, M. A. A.; Lesel, B. K.; Shea, K. J. *Angew. Chem., Int. Ed.* **2014**, *53*, 9275−9279.

(6) (a) Dong, S.; Zheng, B.; Wang, F.; Huang, F. *Acc. Chem. Res.* **2014**, *47*, 1982−1994. (b) Yang, L.; Tan, X.; Wang, Z.; Zhang, X. *Chem. Rev.* **2015**, *115*, 7196−7239.

(7) (a) Yu, C.; Wang, C.-F.; Chen, S. *Adv. Funct. Mater.* **2014**, *24*, 1235−1242. (b) Chen, H.; Ma, X.; Wu, S.; Tian, H. *Angew. Chem., Int. Ed.* **2014**, *53*, 14149−14152.

(8) Dionisio, M.; Ricci, L.; Pecchini, G.; Masseroni, D.; Ruggeri, G.; Cristofolini, L.; Rampazzo, E.; Dalcanale, E. *Macromolecules* **2014**, *47*, 632−638.

(9) Kakuta, T.; Takashima, Y.; Sano, T.; Nakamura, T.; Kobayashi, Y.; Yamaguchi, H.; Harada, A. *Macromolecules* **2015**, *48*, 732−738.

(10) Sambe, L.; de La Rosa, V. R.; Belal, K.; Stoffelbach, F.; Lyskawa, J.; Delattre, F.; Bria, M.; Cooke, G.; Hoogenboom, R.; Woisel, P. *Angew. Chem., Int. Ed.* **2014**, *53*, 5044−5048.

(11) Peters, O.; Ritter, H. *Angew. Chem., Int. Ed.* **2013**, *52*, 8961−8963.

(12) Takashima, Y.; Hatanaka, S.; Otsubo, M.; Nakahata, M.; Kakuta, T.; Hashidzume, A.; Yamaguchi, H.; Harada, A. *Nat. Commun.* **2012**, *3*, 1270.

(13) (a) Nakahata, M.; Takashima, Y.; Hashidzume, A.; Harada, A. *Angew. Chem., Int. Ed.* **2013**, *52*, 5731−5735. (b) Miyamae, K.; Nakahata, M.; Takashima, Y.; Harada, A. *Angew. Chem., Int. Ed.* **2015**, *54*, 8984−8987.

(14) (a) Ogoshi, T.; Kanai, S.; Fujinami, S.; Yamagishi, T.-A.; Nakamoto, Y. *J. Am. Chem. Soc.* **2008**, *130*, 5022−5023. (b) Cao, D.; Kou, Y.; Liang, J.; Chen, Z.; Wang, L.; Meier, H. *Angew. Chem., Int. Ed.* **2009**, *48*, 9721−9723. (c) Xue, M.; Yang, Y.; Chi, X.; Zhang, Z.; Huang, F. *Acc. Chem. Res.* **2012**, *45*, 1294−1308. (d) Strutt, N. L.; Zhang, H.; Schneebeli, S. T.; Stoddart, J. F. *Acc. Chem. Res.* **2014**, *47*, 2631−2642. (e) Wu, X.; Duan, Q.; Ni, M.; Hu, X.; Wang, L. *Youji Huaxue* **2014**, *34*, 437−449.

(15) (a) Yu, G.; Xue, M.; Zhang, Z.; Li, J.; Han, C.; Huang, F. *J. Am. Chem. Soc.* **2012**, *134*, 13248−13251. (b) Duan, Q.; Cao, Y.; Li, Y.; Hu, X.; Xiao, T.; Lin, C.; Pan, Y.; Wang, L. *J. Am. Chem. Soc.* **2013**, *135*, 10542−10549. (c) Cao, Y.; Hu, X.-Y.; Li, Y.; Zou, X.; Xiong, S.; Lin, C.; Shen, Y.-Z.; Wang, L. *J. Am. Chem. Soc.* **2014**, *136*, 10762−10769.

(16) (a) Xia, W.; Hu, X.-Y.; Chen, Y.; Lin, C.; Wang, L. *Chem. Commun.* **2013**, *49*, 5085−5087. (b) Xia, W.; Ni, M.; Yao, C.; Wang, X.; Chen, D.; Lin, C.; Hu, X.-Y.; Wang, L. *Macromolecules* **2015**, *48*, 4403−4409.

(17) (a) Matsue, T.; Evans, D. H.; Osa, T.; Kobayashi, N. *J. Am. Chem. Soc.* **1985**, *107*, 3411−3417. (b) Inoue, Y.; Kuad, P.; Okumura, Y.; Takashima, Y.; Yamaguchi, H.; Harada, A. *J. Am. Chem. Soc.* **2007**, *129*, 6396−6397.

(18) Bitterwolf, T. E.; Ling, A. C. *J. Organomet. Chem.* **1972**, *40*, C29−C32.

(19) (a) Ahn, Y.; Jang, Y.; Selvapalam, N.; Yun, G.; Kim, K. *Angew. Chem., Int. Ed.* **2013**, *52*, 3140−3144. (b) Nakahata, M.; Takashima, Y.; Harada, A. *Angew. Chem., Int. Ed.* **2014**, *53*, 3617−3621. (c) Peng, L.; Feng, A.; Huo, M.; Yuan, J. *Chem. Commun.* **2014**, *50*, 13005−13014.

(20) Venault, A.; Zheng, Y.-S.; Chinnathambi, A.; Alharbi, S. A.; Ho, H.-T.; Chang, Y.; Chang, Y. *Langmuir* **2015**, *31*, 2861−2869.

(21) Yu, G.; Zhou, X.; Zhang, Z.; Han, C.; Mao, Z.; Gao, C.; Huang, F. *J. Am. Chem. Soc.* **2012**, *134*, 19489−19497.

(22) Park, C.; Jeong, E. S.; Lee, K. J.; Moon, H. R.; Kim, K. T. *Chem. - Asian J.* **2014**, *9*, 2761−2764.

(23) Gallei, M.; Schmidt, B. V. K. J.; Klein, R.; Rehahn, M. *Macromol. Rapid Commun.* **2009**, *30*, 1463−1469.

(24) (a) Philippon, A.; Degueil-Castaing, M.; Beckwith, A. L. J.; Maillard, B. *J. Org. Chem.* **1998**, *63*, 6814−6819. (b) Shim, M. S.; Kwon, Y. J. *Biomaterials* **2011**, *32*, 4009−4020.

(25) Alconcel, S. N. S.; Kim, S. H.; Tao, L.; Maynard, H. D. *Macromol. Rapid Commun.* **2013**, *34*, 983−989.

(26) Moon, K.; Kaifer, A. E. *Org. Lett.* **2004**, *6*, 185−188.

DOI: 10.1021/jacs.6b03296
J. Am. Chem. Soc. 2016, 138, 6643−6649